

The NASA Optical Communications and Sensor Demonstration Program: Proximity Operations

Darren Rowen, Siegfried Janson, Chris Coffman, Richard Welle, David Hinkley, Brian Hardy, and Joseph Gangestad
 The Aerospace Corporation
 El Segundo, CA, 90245; 310.336.3633
 Darren.w.rowen@aero.org

ABSTRACT

The Optical Communications and Sensors Demonstration (OCSD) program was initiated in 2012 by NASA's Small Spacecraft Technology Program (SSTP) to demonstrate optical communications from low Earth orbit to small ground terminals, proximity operations using CubeSats, and a CubeSat-compatible thruster. A risk-reduction "Pathfinder" spacecraft (AeroCube OCSD-A) was launched in October, 2015, followed by the main flight units (AeroCubes OCSD-B and -C) in November of 2017. As of June 2018, the -B and -C CubeSats were busy demonstrating the mission goals. Proximity operations started with both CubeSats being brought together within 6 km in the same orbit using a steam thruster. The OCSD-B CubeSat was put into an elliptical co-orbit about the -C CubeSat, with a small along-track drift, using the steam thruster. We performed one pass with a minimum range of 151-meters based on high-accuracy GPS data logged by both spacecraft, plus multiple subsequent passes. Future passes will add imaging and active optical ranging between spacecraft. This paper reviews the thruster system and current proximity operations test results.

INTRODUCTION

The Optical Communication and Sensor Demonstration was funded by NASA's Small Spacecraft Technology Program (SSTP) under the Space Technology Mission Directorate in 2012. The original goals were to demonstrate satellite-to-ground laser communications from a CubeSat with a data rate greater than 5 Mbps, to demonstrate proximity operations using two identical spacecraft, and to demonstrate a CubeSat-compatible thruster. This effort evolved in 2015 from a two-CubeSat flight demonstration into a three CubeSat effort by first launching the qualification model as a pathfinder to test new technologies and uncover hardware or software issues. "Test as you fly" is an accepted risk-reduction methodology; we adopted "fly as you fly" as a new risk-reduction technique that takes advantage of the ten or more CubeSat launch opportunities per year. The pathfinder vehicle (AeroCube-OCSD-A) was launched in October 2015, and we discovered a flaw in our on-orbit reprogramming technique that led to the loss of three-axis attitude control. The vehicle was, and is, functional and we were able to test critical subsystems including the star tracker imaging system, power system, and secondary radio. We had sufficient time to implement software and hardware fixes in the two flight units (AeroCubes-OCSD-B & -C) that were launched in November 2017. Multiple papers chronicle the evolution of this NASA-sponsored effort.^{1,2,3,4,5}

AEROCUBE-OCSD-B & -C SPACECRAFT

Figure 1 is a photograph of AeroCube-OCSD-B with undeployed solar arrays, and Figure 2 is an exploded view graphic of the spacecraft with solar panels fully deployed. AeroCube-OCSD-B is a 1.5U CubeSat with a 2-W output downlink laser at 1064-nm wavelength with a 0.05° FWHM angular beamwidth, an uplink laser receiver/quadcell, two independent 915 MHz communications transceivers, a GPS receiver, a 3-axis attitude control system designed for better than 0.15° pointing accuracy, a laser rangefinder, a corner cube reflector on each face, a 10 megapixel color camera with 180° field of view, a 10 megapixel proximity operations color camera, a 10 megapixel color camera with a 14° field of view for Earth observation, two deployable solar panels, three blue LED beacons, and a distributed computing system composed of over 20 microprocessors and 3 field-programmable gate arrays (FPGAs). An 8-gigabyte flash RAM memory card is used for data storage. The attitude control system has six two-axis sun sensors, four Earth horizon sensors, an Earth nadir sensor, two sets of three-axis magnetometers, two three-axis rate gyros, three magnetic torque rods, three reaction wheels, and two star trackers. AeroCube-OCSD-C is a copy of the -B spacecraft, but with a wider 0.15° FWHM angular beamwidth for the downlink laser. Both spacecraft have a mass of 2.31 kg.

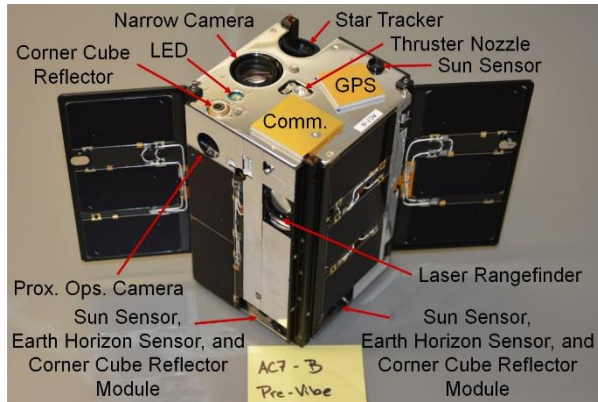


Figure 1: AeroCube-OCSD-B with deployed solar panels.

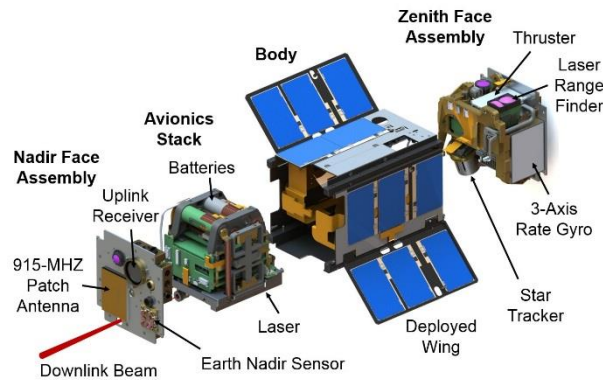


Figure 2: Schematic exploded view of AeroCube-OCSD-B with deployed solar panels.

DEPLOYMENT INTO ORBIT

Figure 3 is a photo of OCSD-B & -C ready for integration into an orbital deployer. Note that one is still being charged to top off the batteries. Both CubeSats occupied the same dispenser, and were sent into orbit on November 12, 2017 from Wallops Island, Virginia on the CRS-8 Cygnus resupply mission to the International Space Station. The Cygnus vehicle undocked with the ISS on December 5, 2017, increased orbit altitude to 450-km circular, and deployed 12 CubeSats, plus AeroCube-OCSD-B & -C on December 7. This initial altitude gives our spacecraft about 2-years of orbital lifetime for laser communications and proximity operations tests.

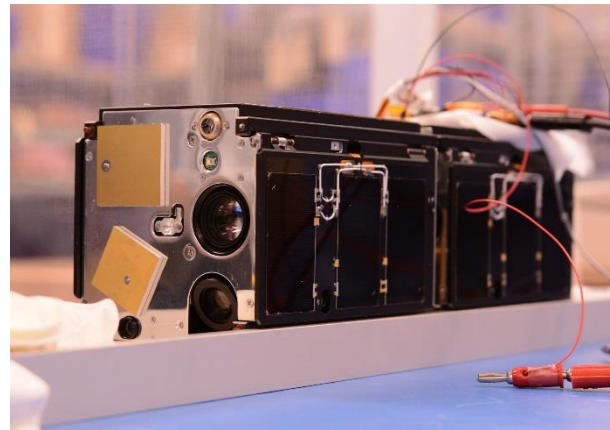


Figure 3: AeroCubes-OCSD-B and -C ready for integration into an orbital deployer.

STEAM THRUSTER SELECTION AND ISSUES

A steam thruster was chosen by the Principal Investigator in 2013 after interactions with NASA safety engineers during the preliminary design review. There were no toxicity, flammability, or carcinogenic issues, no explosion hazards, and the system did not require a pressure vessel for propellant storage. It therefore met the CubeSat specifications without requiring a waiver. In addition, water has a low molecular weight, and the calculated specific impulse of 90s for a 10:1 expansion from a 40° C plenum was much higher than that for butane or any Freon.

A challenging feature of the steam thruster is that it's an evaporating liquid thruster that requires a heat input of 2.9 W/mN to support continuous thrust. This is the heating rate required to vaporize water at the required mass flow rate needed to generate a given thrust level. In addition, according to one-dimensional isentropic expansion calculations, the propellant tank has to maintain a 45°C minimum temperature to prevent vapor freezing before it reaches the 700-micron diameter nozzle throat. Liquid entrainment and freezing have been major issues in thruster design, testing, and on-orbit operation.

The first known on-orbit steam thruster test occurred in February, 2004 on the UK-DMC microsatellite. The spacecraft and thruster were designed and built by Surrey Satellite Technology Ltd. (SSTL) in the United Kingdom. A 10-cm long, 8-mm internal diameter tubular propellant tank was filled with 2.06 grams of water and heated to 200°C.⁶ Ground testing revealed a number of issues such as ice plug formation and rapid ejection of propellant mass, but the limited schedule allowed only one modification: using a sonic orifice instead of a converging/diverging nozzle to prevent ice

buildup in the nozzle expansion region. The first on-orbit thruster test generated 3.3 mN of thrust over 10 cycles using a 0.1 s “on” / 0.9 s “off” duty cycle, and the nozzle temperature dropped by 25 °C. The calculated thrust level for gas-only ejection was 0.2 mN. Liquid water was flowing through the thruster nozzle, yielding a specific impulse of only 5 s, compared to an expected 50 s using a sonic orifice nozzle. The second test, 10 days later, produced no thrust.

SSTL flew a butane thruster on the SNAP-1 nanosatellite with a similar on-orbit problem with expelling some liquid with gas, at least for initial thrusting.⁷ As a result, thrust levels for the first 20 seconds of operation were higher than normal, and the total mission ΔV was reduced to 60% of expected.⁸

The last steam thruster put into orbit was a water/alcohol resistojet on the University of Surrey Space Center Surrey Training, Research, and Nanosatellite Demonstrator (STRaND-1) CubeSat on February 25, 2013.^{9,10,11} Downlink was lost a little more than a month later, on March 30, 2013, and no resistojet flight performance data have been reported.

Figure 4 is a photograph of the OCS D steam thruster. The structure is fabricated in plastic using additive manufacturing, but the nozzle is machined in aluminum to provide smooth surfaces at the 20-micron size scale. Engineering challenges that we overcame included sensor and feed-through corrosion by water, thermal control and insulation, and ice plugs that formed during the first few firings in vacuum.

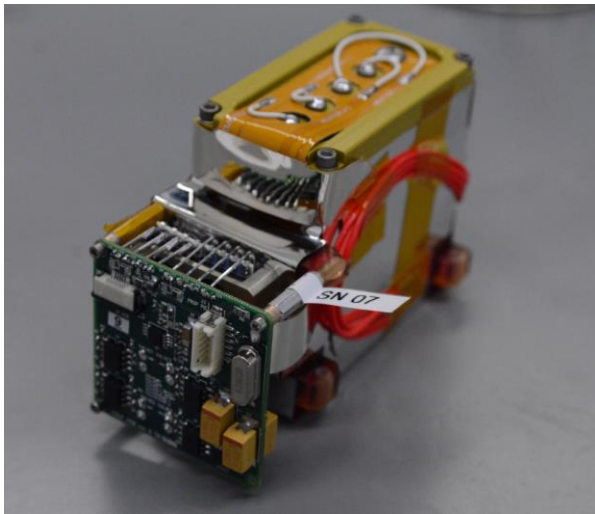


Figure 4: The steam thruster module.

GROUND TESTS OF OUR STEAM THRUSTER

Figure 5 is a photograph of a ~2-cm high ice plug that formed above the nozzle exit during a ground test. Ice plugs typically form during the first few test firings in vacuum when liquid water is ejected into vacuum. We filled our propellant tanks at ambient pressure using a water-filled syringe. When sealed, the internal plenum pressure is 1 atmosphere; much higher than the 0.07 to 0.11 bar pressure range for water vapor between 40 and 48 °C. To limit ejection of liquid water, we limited filled water volume to 26 cc. This increased the ullage fraction. In addition, thrusters were briefly test fired in a vacuum to vent excess air pressure before further environmental testing and integration of these thrusters into flight spacecraft.

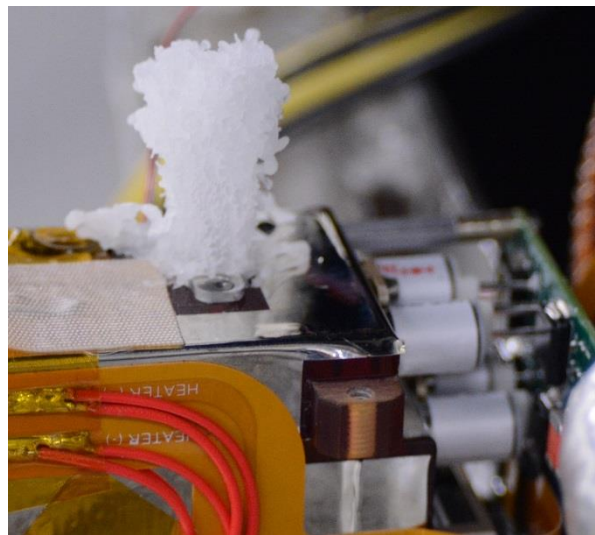


Figure 5: Ice plug buildup by the steam thruster firing in a vacuum.

All flight thrusters were thermally-cycled from +61 to -24°C for 20+ cycles, and their mass and internal pressure were monitored after each test to uncover leaks. A thermal bake out test of 6 hours under vacuum at pressures below 10^{-4} Torr at 60°C yielded a post-test mass loss of only 0.02 grams for one unit, and 0.06 grams for the second unit. These minor mass losses were attributed to outgassing and not propellant loss. Both units were subjected to vibration testing at general environmental vibration specification (GEVS) 14.1-g rms levels for one minute at each axis, with no issues.

Figure 6 plots measured thrust levels in vacuum produced by serial number 08 steam thruster module, operating with a body and exit nozzle temperature of 40°C, and valve open times of 50, 250, and 1000 milliseconds, respectively. The thruster was put on a digital weight scale, with the nozzle pointing up, in a vacuum chamber. Measured force is the weight of the

module, plus any offset, plus thrust. Thrust is determined by subtracting the baseline from the instantaneous force measurement. The impulse bit for the 50 and 250 millisecond valve opening times are 0.2 and 0.6 mN-s, respectively. At 1000 milliseconds, the impulse bit increases to 2.8 mN-s. For open times greater than 1.5 seconds, the impulse bit scales as 3.0 mN times the valve open time.

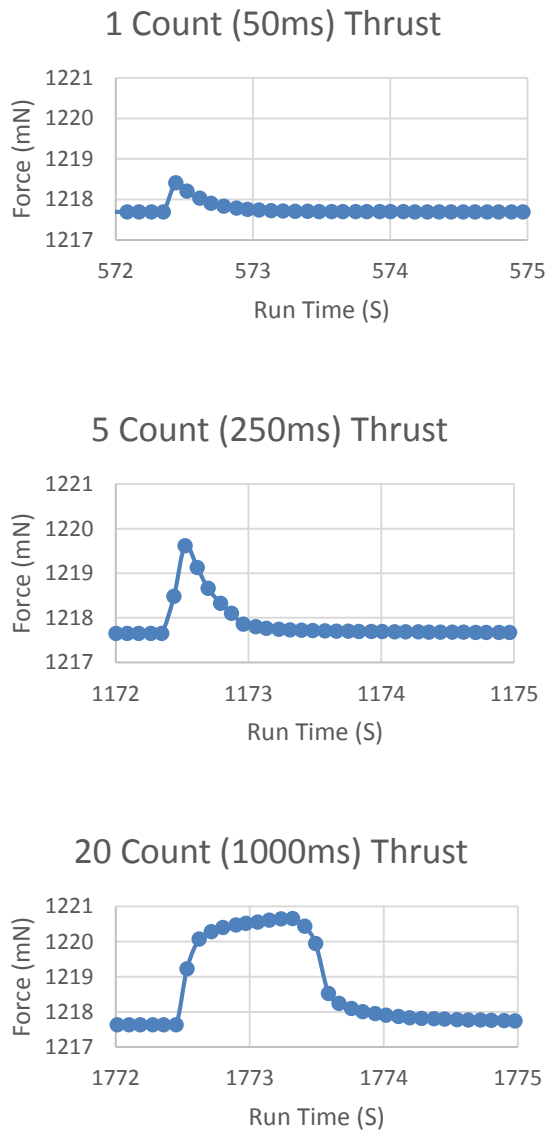


Figure 6: Thrust levels in vacuum measured by an electronic scale.

ON-ORBIT TESTS OF OUR STEAM THRUSTER

Thruster firings on both spacecraft were attempted in late January, 2018. The initial attempts showed no thrust and

tank pressures in excess of 500 mbars. We suspected rapid liquid ejection due to the high tank pressure, with subsequent ice plug formation similar to what we observed in ground testing. We increased thruster temperature to 48 °C, and turned the spacecraft so that the sun heated the thruster nozzle. After 30 seconds of cumulative thruster operation under these conditions, tank pressure had dropped to the vapor pressure of water. The AeroCube-OCSD-B thruster system was ready for orbit modification maneuvers on February 25, 2018, and the -C system was ready on March 3. Thruster temperature for all future maneuvers was increased to 48 °C to minimize ice formation in the nozzle.

PROXIMITY OPERATIONS

On March 15, the -B CubeSat was commanded to thrust in an initial attempt to reduce the separation rate between both CubeSats. They had been ejected by the same deployer and had the same mass and dimensions, but they were separating at a rate of 11.7 km/day due to the impulse imparted by the separation springs between the two CubeSats and cumulative differences in ballistic coefficient caused by differing orientations. Our original plan was to use differential air drag, but firing a thruster was faster, did not interfere with on-going optical downlink tests, and reduced mission risk. Lower risk resulted from eliminating the need to keep both spacecraft active for days on end while maintaining a fixed attitude with respect to the flight direction. Our normal mode of operation is to let most spacecraft systems sleep, including attitude control, until needed for experiments, taking GPS fixes, etc. The additional propellant usage, 130 milligrams, was minimal; 0.5% of the propellant stored on one spacecraft.

Figure 7 is a plot of in-track separation between the two CubeSats calculated using high-accuracy ephemerides determined by least-squares fitting to 9 separate position and velocity determinations, per orbit, by the on-board GPS receiver before and after thruster firing. The separation rate after the burn was reduced to 4.60 km/day; this represented an imparted ΔV of 2.7 cm/s.

The next burn by AeroCube-OCSD-B, on March 22, reversed the separation and caused both spacecraft to approach each other at a rate of 2.2 km/day. Figure 8 is a plot of the calculated separation of both spacecraft as a function of time after 9 seconds of thruster firing at 48 °C.

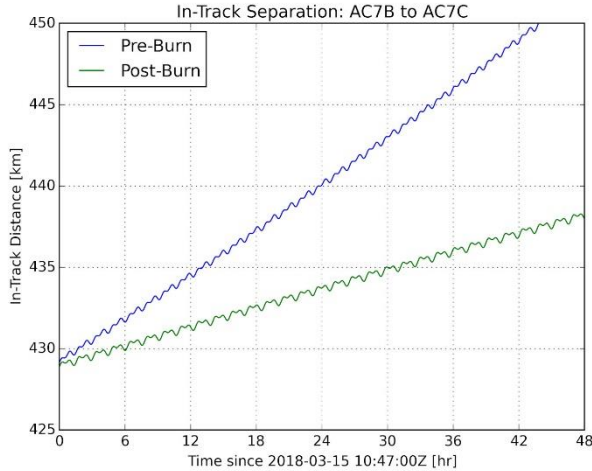


Figure 7: In-track separation between AeroCube-OCSD-B and -C based on orbital elements before and after the first proximity operations burn.

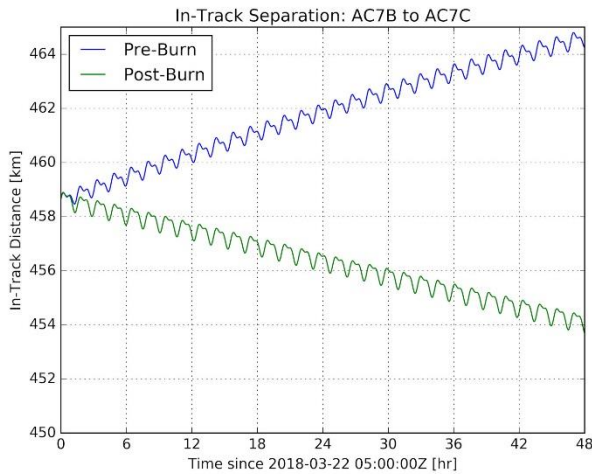


Figure 8: In-track separation between AeroCube-OCSD-B and -C based on orbital elements before and after the second proximity operations burn.

The change in separation rate shown in Fig. 8 was -5.9 cm/s, corresponding to an imparted ΔV of ~ 2.0 cm/s. The expected ΔV was 1.8 cm/s. The measured and expected ΔV s are 10% different, but within our measurement errors. At this post-burn rate of approach, it would take 209 days to bring the spacecraft together.

Multiple firings occurred in April and May to adjust the approach rate and attempt a first stop at ~ 10 km range, and later at ~ 5 km range. Figure 9 is a plot of the in-track separation between the two spacecraft resulting from the thrusting maneuver that put AeroCube-OCSD-B on a trajectory to pass AeroCube-OCSD-C located at 0 km in-track distance. The ripples in this graph, and all previous range graphs, are due to slight differences in

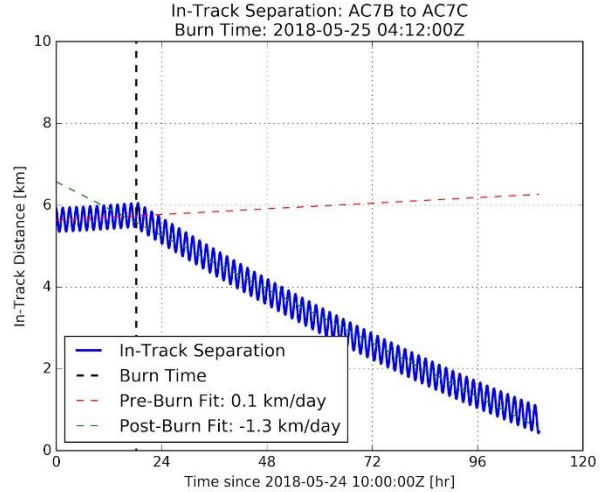


Figure 9: In-track separation between AeroCube-OCSD-B and -C based on orbital elements before and after the first proximity operations interception burn.

orbit eccentricity, semi-major axis, orbit inclination, etc., between both spacecraft. Each ripple period in Fig. 9 is an orbit period.

Our proximity operations plan was to insert one spacecraft into a co-orbital corkscrew orbit about the other, and let them slowly drift together and apart. Once properly set up with sufficient co-orbital radii, both spacecraft can be left unattended for days with little risk of collision. Figure 10 is a plot of range between spacecraft, before, during, and after closest approach on May 29. The minimum range was 151 meters!

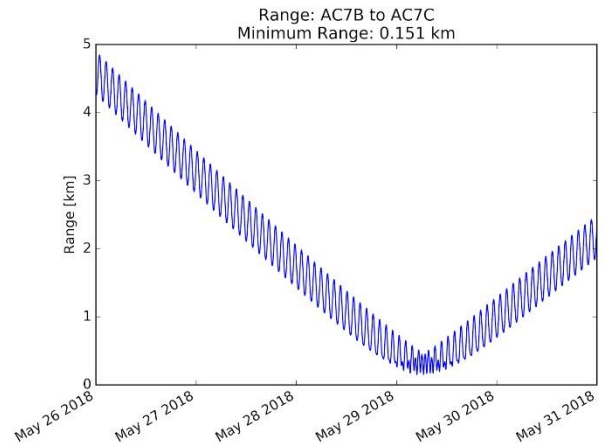


Figure 10: Range between AeroCube-OCSD-B and -C based on GPS-derived orbital elements obtained during the encounter phase.

The sinusoidal oscillations in Figs. 9 and 10 indicate that the corkscrew orbit of AeroCube-OCSD-B was centered

about the orbit of AeroCube-OCSD-C. Figure 11 shows the relative radial and cross-track motion of the -B CubeSat relative to the -C CubeSat, and the cross sections of the relative corkscrew co-orbit. The propulsive maneuver on May 9 (Fig. 9) was set up perfectly; the -C spacecraft was in the middle of the radial and cross-track ellipse.

Figure 12 shows the return burn that set up another proximity flyby on June 3, 2018 at a “leisurely” 800 meters per day. To date, we have performed two more proximity flybys, and are preparing to test camera acquisition of blinking LEDs on the other spacecraft. We also plan to use the laser rangefinder on each CubeSat to provide real-time data. The laser range accuracy is better than 1 meter, while the current GPS-fed high-accuracy ephemerides are limited to ~5 meter accuracy.

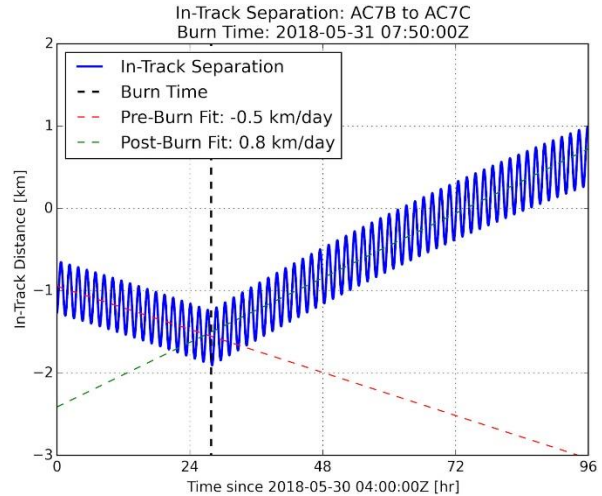


Figure 12. May 31 burn to setup a second flyby of AeroCube-OCSD-B with -C.

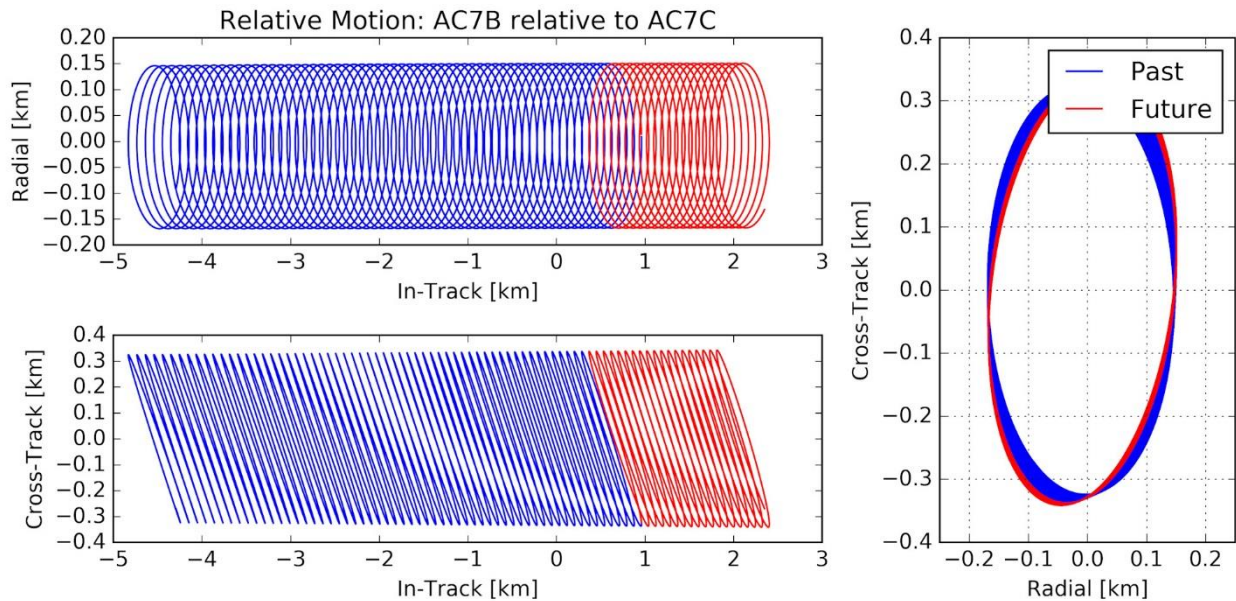


Figure 11. Radial, cross-track, and in-track inter-satellite distances for the first proximity flyby based on on-orbit GPS data. The plot was created for 01:00:00 UTC on March 31, 2018.

STATUS

We have demonstrated the first OCSD proximity operations goal of flying one CubeSat past another in a helical co-orbit that minimizes the risk of collision between both spacecraft. We wanted to perform proximity operations without increasing the orbital

debris population, and we believe these are the first CubeSats to perform this proximity operations maneuver. Proximity operations was enabled by an on-board GPS receiver and a 3-axis attitude control system with better than 0.05° pointing accuracy, originally developed for the express purpose of aiming a laser downlink in each Cubesat. It was also enabled by

development of a simple steam thruster that meets CubeSat specifications, and poses minimum risk for CubeSat developers and launch vehicles. We had to vent excess pressure once on orbit, and operate at slightly higher temperatures than originally planned. Impulse bits generated by this thruster on orbit have not scaled reliably with valve “on” time and we are still trying to understand the mechanisms at work. Our next goal is to actively locate each spacecraft during a proximity operations maneuver using a color imager and flashing blue LED beacons on each CubeSat, and take range measurements using the on-board laser rangefinders. The imager should be able to see the other OCSD CubeSat at a 10 km range, and the laser rangefinder has been tested at a 2.25-km range on the ground.

References:

1. Janson, S.W., and R.P. Welle, “The NASA Optical Communication and Sensor Demonstration Program,” paper SSC13-II-1, AIAA/USU Small Satellite Conference, Logan, Utah, August 10-15, 2013.
2. Janson, Siegfried W., and Richard P. Welle, “The NASA Optical Communication and Sensor Demonstration Program: An Update,” paper SSC14-VI-1, 28th AIAA/USU Small Satellite Conference, Logan, Utah, August, 2014.
3. Rose, T.S. et al., “LEO to Ground Optical Communications from a Small Satellite Platform,” *Proc. SPIE 9354*, Free Space Laser Communication and Atmospheric Propagation XXVII, 935401, March, 2015.
4. Janson, Siegfried W., et al., “The NASA Optical Communication and Sensors Demonstration Program: Preflight Update,” paper SSC15-III-1, 29th Annual AIAA/USU Conference on Small Satellites, Logan, Utah, August 2015.
5. Janson, Siegfried. et al., “The NASA Optical Communication and Sensors Demonstration Program: Initial Flight Results,” paper SSC16-III-03, 30th Annual AIAA/USU Conference on Small Satellites, Logan, Utah, August 2016.
6. Gibbon, D., et al., “The Design, Development, and In-Flight Operation of a Water Resistojet Micropropulsion System,” paper AIAA 2004-3798, 40th AIAA/ASME/SAE/ASEE Joint Propulsion Conference and Exhibit, Ft. Lauderdale, Florida, July 11-14, 2004.
7. Underwood, Craig L., “The UK’s First Nanosatellite: SNAP-1,” pp.297-325, Chapter 10 in *Small Satellites: Past, Present, and Future*, American Institute of Aeronautics and Astronautics, Inc., Reston, Virginia, USA, 2008.
8. Gibbon, D., and C. Underwood, “Low Cost Butane Propulsion System for Small Spacecraft,” paper SSC01-XI-1, 15th Annual AIAA/USU Conference on Small Satellites, Logan, Utah, August, 2001.
9. Satnews, “Satnews Daily” web page for Feb. 25, 2013, URL: <http://www.satnews.com/story.php?number=1867923907> , retrieved June, 2018.
10. American Institute of Aeronautics and Astronautics, “Dancing CubeSats,” *Aerospace America*, July/August 2017, URL: <https://aerospaceamerica.aiaa.org/features/dancing-cubesats/> , retrieved June, 2018.
11. Bridges, C.P. et al., “A Baptism of Fire: The STRaND-1 Nanosatellite,” paper SSC13-X-3, 27th Annual AIAA/USU Conference on Small Satellites, Logan, Utah, August, 2013.

Acknowledgements

We want to thank NASA’s Small Spacecraft Technology Program (SSTP) for funding this work, and the NASA-Ames Research Laboratory for managing the program. We would also like to thank the 50+ engineers and scientists at The Aerospace Corporation that provided the needed expertise and effort required to make this program a success.